



OPEN Nuclear protein 1 is a cell death regulator in primary human airway epithelial cells and reduced in idiopathic pulmonary fibrosis

Marie Zöller¹, Michal Mastalerz¹, Elisabeth Dick¹, Juliane Merl-Pham², Elisabeth Hennen¹, Sai Rama Sridatta Prakki³, Ashesh Chakraborty¹, Misako Nakayama¹, Markus Klotz¹, Hannah Marchi⁴, Ronan LeGleut⁴, Laurens J. De Sadeleer⁵, Wim A. Wuyts⁵, Bart M. Vanaudenaerde⁵, Aicha Jeridi¹, Antje Prasse⁶, Benedikt Jäger⁶, Patricia Santofimia-Castaño⁷, Mircea-Gabriel Stoleriu¹, Anne Hilgendorff¹, Stefanie M. Hauck², Ali Ö. Yildirim^{1,8}, Herbert Schiller^{3,8} & Claudia A. Staab-Weijnitz^{1,9}✉

The airway epithelium is the first site of injury from cigarette smoke (CS), a major risk factor for chronic lung disease including idiopathic pulmonary fibrosis (IPF). Here, we report the first intracellular proteomic analysis of CS exposure in fully differentiated primary human bronchial epithelial cells (phBECs). Following pathway enrichment analysis, we identified nuclear protein 1 (NUPR1) as a candidate regulator of epithelial stress responses. In contrast to the prediction by pathway enrichment analysis, NUPR1 activity was not altered by CS *in vitro*. Nevertheless, inhibition of its nuclear translocation using ZZW-115 revealed a cytoprotective and anti-apoptotic role in phBECs, as demonstrated by increased apoptosis and impaired epithelial integrity. *NUPR1* expression was markedly reduced in IPF whole lung tissue and bronchial epithelium. IPF-derived basal cells differentiated into an epithelium exhibiting fewer ciliated and more secretory cells which exhibited significantly higher sensitivity to NUPR1 inhibition. Our findings underscore cell type- and tissue-specific variation in NUPR1-dependent pathways. Collectively, this study positions NUPR1 as a context-dependent epithelial stress regulator whose loss may contribute to epithelial vulnerability in IPF.

Keywords NUPR1, Cigarette smoke, Bronchial epithelium, IPF, ALI culture, *In vitro*

Idiopathic pulmonary fibrosis (IPF) is a chronic progressive fibrotic interstitial lung disease, which is occurring predominantly in middle aged or older male individuals^{1,2}. The disease is characterized by chronic cough, progressive dyspnoea, and ultimately failure of lung function, leading to high mortality rates^{1,3}. The median survival is 3–5 years after diagnosis and incidences worldwide are increasing³. Although the progression can be slowed down using the anti-fibrotic drugs nintedanib⁴, pirfenidone⁵, and nerandomilast⁶, no curative treatment is yet available. Due to the advanced age of IPF patients and high prevalence of comorbidities, lung transplantations are often contraindicated¹. Therefore, novel therapeutic options are urgently needed.

While the precise aetiology of IPF remains unknown, cigarette smoke (CS) is increasingly recognized as a major risk factor in its pathogenesis^{1,3,7–9}. 41–83% of IPF patients have a smoking history^{8,10–12}. Previous studies

¹Comprehensive Pneumology Center with the CPC-M bioArchive and Institute of Lung Health and Immunity, Member of the German Center of Lung Research (DZL), Helmholtz-Zentrum München, Munich, Germany.

²Metabolomics and Proteomics Core, Helmholtz Munich, Munich, Germany. ³Research Unit Precision Regenerative Medicine, Comprehensive Pneumology Center, Helmholtz Munich, Munich, Germany. ⁴Core Facility Statistical Consulting, Helmholtz Munich, Munich, Germany. ⁵Laboratory of Respiratory Diseases and Thoracic Surgery (BREATHE), Department Chrometa, KU Leuven, Leuven, Belgium. ⁶Department of Pulmonology, Fraunhofer Institute for Toxicology and Experimental Medicine, Hannover, Germany. ⁷Pancreatic Cancer, Cancer Research Centre of Marseille, Institute Paoli-Calmettes, Aix-Marseille University, Marseille, France. ⁸Institute of Experimental Pneumology, LMU University Hospital, Ludwig-Maximilians University, Munich, Germany. ⁹Department of Pediatrics and Division of Pulmonary, Allergy and Critical Care Medicine, School of Medicine, University of Colorado Anschutz Medical Campus, Aurora, CO, USA. ✉email: claudia.staab-weijnitz@cuanschutz.edu

estimated that adults with a smoking history have a 60% higher lifetime risk to develop IPF¹¹. Furthermore, there is a dose- and intensity-dependent correlation between smoking and the risk of IPF development⁷. CS contains more than 4000 chemical compounds and is responsible for the premature death of up to half of active smokers^{13,14}. It contributes to the development of various pulmonary diseases, cardiovascular disease and lung cancer^{11,15}, causing over 8 million deaths annually^{15–17}. This makes smoking one of the most serious threats to public health¹⁴.

The bronchial epithelium is a pseudostratified layer of cells lining the tracheobronchial tree. It is mainly composed of basal, club, goblet and ciliated cells^{13,18,19}. Basal cells act as stem cells of the airway, essential for epithelial regeneration and differentiation into all cell types within the lung epithelium. Ciliated and goblet cells are responsible for mucociliary clearance to remove harmful particles. Mucus is mainly produced by goblet cells. Club cells are the progenitor cells of ciliated and goblet cells. They provide secretory surfactants and uteroglobin (CC10), which has an anti-inflammatory function^{18,20}. Moreover, cytochrome P450 enzymes are abundantly expressed in club cells which mediate the detoxification of inhaled xenobiotics²¹. The airway epithelium is the major portal of entry for inhaled toxins, particles and pathogens, including CS, wood dust and herpesvirus infection which are linked to the aetiology of IPF^{22,23}. It is well known that the composition of the bronchial epithelium can be altered due to lung disease^{18,24}. In recent studies increasing attention has been brought towards the emerging role of the airway epithelium in the pathogenesis of IPF. Most strikingly, a common single nucleotide polymorphism (SNP) in the promoter region of the gene encoding mucin 5B (*MUC5B*) conveys by far the greatest genetic risk to develop IPF²⁵. In IPF, *MUC5B* expression is common in distal airway epithelial cells, including transitional zones between bronchioles and alveoli, areas of bronchiolization, and honeycomb cysts, and associates with impaired mucociliary clearance²⁶. But also proximal airways undergo significant remodelling and functional impairment in IPF²⁴. However, the mechanisms by which airway epithelial cells and CS exposure contribute to IPF development and progression are incompletely understood.

In the present study, we set out to identify novel CS-induced key regulators in differentiated airway epithelial cells using an unbiased proteomics approach followed by pathway enrichment analysis. This predicted Nuclear protein 1 (NUPR1) as a novel key regulator in these cells which prompted us to study the role of NUPR1 in phBECs including those derived from IPF patients. Our results indicate an important general role for NUPR1 in airway epithelial cell death which is little affected by CS exposure *in vitro*. Interestingly, differentiated IPF-derived phBECs were significantly more susceptible to NUPR1 inhibition-induced cytotoxicity. Furthermore, after 28 days of differentiation, IPF-derived phBECs were characterized by a marked reduction in ciliated at the expense of goblet cells compared with control phBECs, indicating that IPF-derived basal cells are reprogrammed to yield an airway epithelium with fewer ciliated and more secretory cells.

Some of the results of this study have been previously reported in the form of a conference abstract²⁷.

Materials and methods

For more details on materials and methods, including primers and antibodies used for gene expression analysis (Supplemental Tables S3–S4), see the online supplement. The mass spectrometry proteomics data have been deposited to the ProteomeXchange Consortium via the PRIDE²⁸ partner repository with the dataset identifier PXD063763.

Patient material

Primary human bronchial epithelial cells (phBECs) from three Idiopathic Pulmonary Fibrosis (IPF) and seven non-chronic lung disease (control) donors were provided by the CPC-M bioArchive (Comprehensive Pneumology Center, Helmholtz Munich). The ethics committee of the Ludwig-Maximilians-University Munich approved this study (ethic votes #333-10) and all participants provided a written informed consent. All research was performed in accordance with the relevant guidelines and regulations. PhBECs were isolated as previously described^{29–31}. Briefly, bronchi were treated with Pronase E and incubated. Epithelial cells were gently scraped with a scalpel, minced and filtered through a 70 mm strainer to remove tissue. The cells were placed on uncoated petri dishes for 3 h to remove fibroblasts. The supernatant was transferred on a collagen I-coated (136157, ChemCruz) petri dish in Pneumacult Ex-Plus media (5040, Stemcell Technologies) containing 1% penicillin–streptomycin (pen/strep, 15140, Gibco). The cells were tested for *Mycoplasma pneumoniae*. The negative tested cells were expanded to passage 1, frozen down and stored in liquid-nitrogen.

One sample of IPF-derived phBECs (donor 7) was obtained from Hannover Medical School. The study was approved by the Institutional Review Boards at Hannover Medical School (approved IRB protocols #2518-2014 and #2923-2015) and University Medical Center Freiburg (approved IRB protocols #239/12 and #03/10). All participants provided a written informed consent. Isolation of phBECs was performed as previously described³².

For the NUPR1 inhibition experiment, control phBECs were derived from histologically normal lung regions of patients undergoing lung tumour resections (two males, two females, mean age 73.25 ± 2.29 years (SEM)). IPF phBECs were derived from airways of IPF patients (three males, one female, mean age 65.25 ± 2.17 years (SEM)). For the proteomics analysis, control phBECs were used (three males, one female, mean age 73.50 ± 2.33 years (SEM)). For more details on patient characteristics, please refer to Supplemental Table S1.

Additionally, formalin-fixed, paraffin-embedded (FFPE) tissue samples of peritumoral tissue from five non-chronic lung disease patients were provided by the CPC-M bioArchive (Comprehensive Pneumology Center, Helmholtz Munich). The ethics committee of the Ludwig-Maximilians-University Munich approved this study (ethic votes #19-630) and all participants provided written informed consent. To obtain control FFPE lung sections, fresh lung tissue specimen of approximately 8 mm³ were fixed in paraformaldehyde (PFA) for over 24 h at room temperature (RT). Subsequently, they were transferred into PBS at 4 °C before the processing in the tissue processor according to the manufacturer's instructions and embedding in paraffin. The paraffin blocks were stored at RT prior to sectioning at a thickness of 5 µm.

FFPE lung sections from five IPF patients were obtained from the KU Leuven lung biobank (ethical approval S52174). All participants provided a written informed consent. The FFPE processing was performed as previously described³³.

For the NUPR1 quantification in lung sections, control FFPE sections were derived from histologically normal lung regions of patients undergoing lung tumour resections (four males, one female, mean age 62.40 ± 5.58 years (SEM)). IPF derived FFPE sections were derived from explanted lungs of IPF patients (four males, one female, mean age 59.80 ± 1.88 years (SEM)). For more details on patient characteristics, please refer to Supplemental Table S2.

NUPR1 inhibition

N,N-dimethyl-4-[3-[2-(trifluoromethyl)-10H-phenothiazin-10-yl]propyl]-1-piperazineethanamine trihydrochloride (ZZW-115, 34,974 /CAS 10122-45-9, Caymen Chemical) was dissolved in dimethyl sulfoxide (DMSO, D4540/ CAS 67-68-5, Sigma-Aldrich) to prepare a 30 mM stock solution. The stock solution was stored at -80 °C in aliquots until further use. For NUPR1 inhibition experiments in phBECs the stock solution was diluted in Pneumacult ALI Basal medium (05,041, Stemcell Technologies) to obtain a final concentration of 0–150 μ M ZZW-115 and 0.5% DMSO. This inhibition solution was applied to both sides of the transwell membrane for 24 h, with 200 μ L added to the apical and 1 mL to the basolateral side.

Results

Proteomic analysis of chronically cigarette smoke extract (CSE)-exposed phBECs confirms known CS-regulated pathways and suggests NUPR1 as a potential novel regulator of the airway epithelial response to CS

Label-free LC-MS/MS-based proteomic analysis of control phBECs of the pooled data of four time points of differentiation (day 7, 14, 21 and 28, see Fig. 1A) detected in total 4861 distinct proteins, out of which 186 were differentially expressed over the whole time course as a result of chronic CSE-exposure ($q < 0.05$). Overall, the magnitude of expression changes was moderate, with most \log_2 fold changes ranging between 1 and -1. This is in qualitative agreement with our previous study using the same culture and CSE exposure approach where CS-induced changes were much more drastic on the transcript than on the protein level³⁰ (Online Supplement 2: “Final Protein List”). The top 50 CSE-regulated proteins according to \log_2 fold changes (Fig. 1B) included, as expected, upregulated enzymes of xenobiotic metabolism (Cytochrome P450 1B1 (CYP1B1), Aldehyde dehydrogenase, dimeric NADP-preferring (ALDH3A1), Aldo-keto reductase family 1 member C1 (AKR1C1), Aldo-keto reductase family 1 member B10 (AKR1B10), NAD(P)H dehydrogenase [quinone] 1 (NQO1)), again confirming our previous findings³⁰. Notably, Selenoprotein H (SELH) and Interleukin 33 (IL33) belonged to the most downregulated proteins and using immuno-based approaches, we confirmed loss of intracellular SELH using ELISA and loss of IL33 using Western Blot analysis (Supplemental Fig. S1–S2). While loss of IL33 was found for all assessed time points, loss of SELH was most pronounced at early time points of differentiation.

Next, we subjected this protein list to pathway enrichment analysis to identify potential novel key regulators of the CS response in the airway epithelium. The proposedly altered pathways included such that are well-established to be affected by CS exposure, including activation of the Aryl hydrocarbon receptor (AhR) signalling pathway³⁴ and downregulation of Sirtuin signalling pathways³⁵ (Fig. 1C). Pathway enrichment analysis suggested 23 key regulators of the CS response (Supplemental Table S5), including known factors like β -catenin³⁶, transforming growth factor β 1³⁷ and KRAS³⁸, while NUPR1, to the best of our knowledge, had not been described in the context of the airway epithelial response to CS (Fig. 1D, E, Supplemental Fig. S3). Therefore, we hypothesized that NUPR1 is activated by CS in phBECs and protects from airway epithelial cell death. With airway-like cells emerging as key players in IPF and CS-induced pathways remaining poorly understood in this context, we further investigated whether NUPR1 acts as a survival factor in IPF-derived airway epithelial cells and whether its expression is changed in IPF.

ZZW-115 efficiently blocks nuclear translocation of NUPR1 and displays dose-dependent cytotoxicity in phBECs

To study the role of the transcription factor NUPR1 in phBECs, fully differentiated phBECs were treated with the NUPR1 specific inhibitor ZZW-115 (0–150 μ M). ZZW-115 prevents the complex formation between NUPR1 and importin, which inhibits the nuclear translocation of NUPR1 and thus NUPR1-induced gene transcription³⁹. IF analysis showed strong cytoplasmic retention of NUPR1 protein and a clear reduction of nuclear NUPR1 in treated cells, confirming target engagement in our system (Fig. 2A). Also, NUPR1 inhibition in phBECs confirmed the regulation of selected NUPR1 target genes as suggested by IPA on transcript level (Fig. 2B–D). Finally, ZZW-115 was cytotoxic to phBECs in a dose-dependent manner with an IC_{50} -value of 63.6 μ M (Fig. 2E). These results validated that ZZW-115 worked efficiently in blocking the nuclear translocation of NUPR1 in our culture model and that inhibition of NUPR1 nuclear translocation induces cell death in phBECs, indicating an important protective role in bronchial epithelial cells.

NUPR1 is expressed in basal and ciliated cells

To identify which cells express NUPR1 in our culture system, we extracted data from an existing scRNA-seq data set from fully differentiated control phBECs⁴¹. This data set suggested ciliated and basal cells as the main NUPR1-expressing cells (Fig. 3A). IF stainings of NUPR1 in combination with cell type-specific markers in control phBECs confirmed the findings of the scRNA-seq analysis in phBECs in vitro, where CC10- and MUC5AC-positive cells, i.e. secretory cells, were always negative for NUPR1 whereas NUPR1-positive cells were positive for p63 (basal cell marker) or acetylated tubulin (ciliated cell marker, Fig. 3B). IF stainings of ZZW-115 treated phBECs showed loss of all cell types due to NUPR1 inhibition induced cytotoxicity (Fig. 3B).

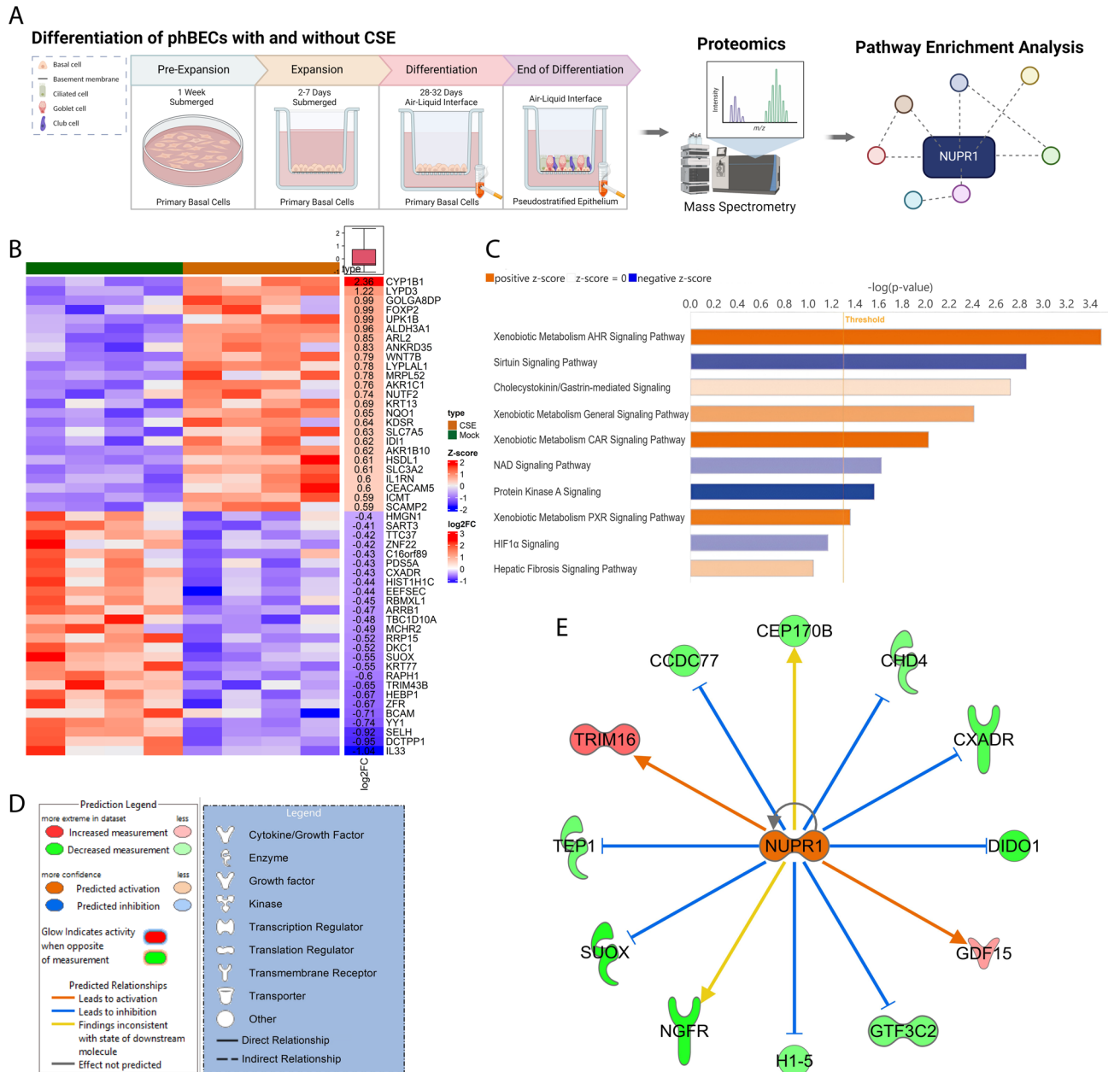


Fig. 1. Experimental set-up for proteomic analysis of cigarette smoke (CS)-induced changes in primary human bronchial epithelial cells (pHBECs). **(A)** Schematic overview of the differentiation of pHBECs, both with and without CS extract at air-liquid interface (ALI). These cells were then submitted to label-free tandem mass spectrometry-based proteomics followed by pathway enrichment analysis(created using Biorender). **(B)** The proteomic data were analysed using a Wald test with Storey’s correction for multiple testing. The heatmap shows protein expression profiles of CS-treated versus control pHBECs (pooled time points of all differentiation days for each donor, $n = 4$). It displays the z-scores of the top 50 CS-induced differentially expressed proteins by \log_2 fold change (Wald test $q < 0.05$). Z-scores were calculated for each protein across the samples to standardize expression levels. Data analysis and visualisation were performed in RStudio. **(C)** Pathway enrichment analysis of the proteomic dataset revealed CS-modulated molecular pathways in pHBECs (orange: activation, blue: inhibition; the colour intensity reflects the magnitude of the z-score with darker shades indicating a higher absolute z-value). **(D)** Legend for ingenuity pathway analysis-derived regulatory molecular network **(E)**. Proposed CS-activated upstream regulators included **(E)** NUPR1 which is shown in the context of altered target proteins within the data set.

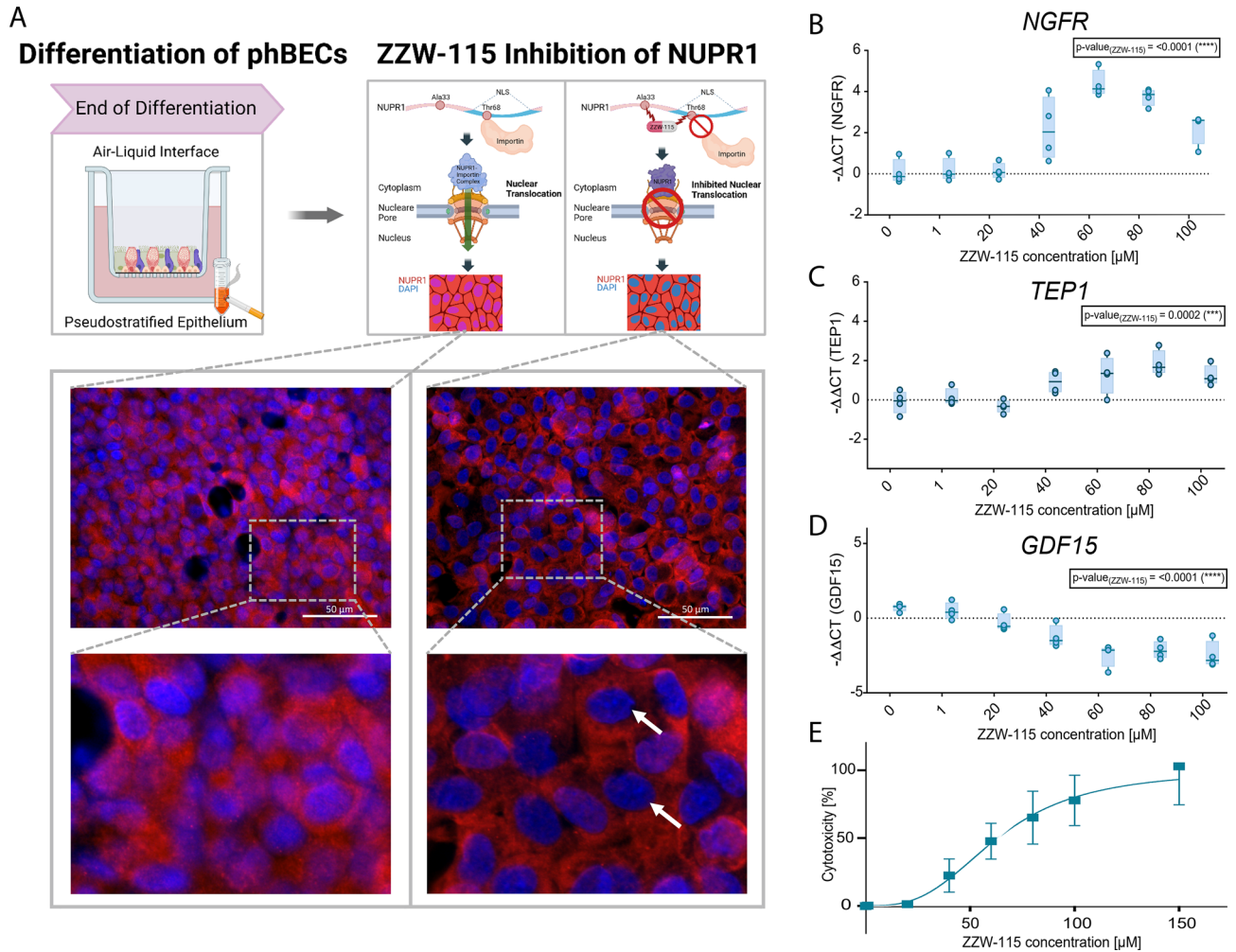


Fig. 2. NUPR1 inhibits nuclear translocation in fully differentiated primary human bronchial epithelial cells (phBECs). **(A)** PhBECs were fully differentiated followed by 24 h of NUPR1 inhibition using ZZW-115 (0–150 μM) both on apical and basolateral side. Inhibition of nuclear translocation of NUPR1 was confirmed by immunofluorescence stainings of phBECs treated with DMSO vehicle control (left) and ZZW-115 at a concentration close to its IC_{50} (60 μM , right; scale bar 50 μm ; created with Biorender; adapted from⁴⁰). **(B–D)** QPCR analysis after 24 h of treatment revealed a significant modulation of IPA-predicted NUPR1-regulated target genes *NGFR*, *TEP1*, *GDF15* due to NUPR1 inhibition in a dose-dependent manner (0–100 μM , $n = 4$). **(E)** Lactate dehydrogenase assay revealed that inhibition of NUPR1 by ZZW-115 increased cytotoxicity in fully differentiated control phBECs ($n = 4$) in a dose-dependent manner ($\text{IC}_{50} = 63.6 \mu\text{M}$). All data is presented as mean \pm SD.

Cigarette smoke exposure does not activate NUPR1 in phBECs

CS is the most important risk factor for chronic lung disease⁴². Given that IPA analysis of our proteomics study suggested the activation of NUPR1 in phBECs by CS (Fig. 1E) and that NUPR1 has been suggested to fulfil a protective role in alveolar epithelial cells in the context of COPD⁴³, we sought to investigate whether CS exposure may activate NUPR1 thus protecting from CS-induced cell death in phBECs.

Western blot analysis of fully differentiated control phBECs ($n = 4$) failed to show consistent changes of NUPR1 protein levels in response to CSE exposure (Fig. 4A, B, Supplemental Fig. S4). Additionally, IF stainings did not show any differences in subcellular localization of NUPR1 after CSE treatment (Fig. 4C). QPCR analysis of ZZW-115 treated (0–100 μM) phBECs revealed no changes in transcript levels of selected IPA-predicted NUPR1 target genes (Tumor necrosis factor receptor superfamily member 16 (*NGFR*), Telomerase protein component 1 (*TEP1*), Growth/differentiation factor 15 (*GDF15*), Centrosomal protein of 170 kDa protein B (*CEP170B*)) upon CSE exposure. However, except for CEP170B, these targets were modulated by NUPR1 inhibition in a dose-dependent manner in both conditions (Fig. 4D–F, Supplemental Fig. S5), confirming them as NUPR1-dependent genes in our culture system. As previously shown in Fig. 2, ZZW-115 induced cytotoxicity to phBECs in a dose-dependent manner. However, CSE exposure did not significantly affect the response, resulting in very similar IC_{50} values ($63.6 \pm 5.1 \mu\text{M}$ without and $63.9 \pm 4.4 \mu\text{M}$ with CSE; Fig. 4G). In addition, cell barrier integrity was significantly reduced by ZZW-115 treatment to a similar extent with and without CSE (Fig. 4H).

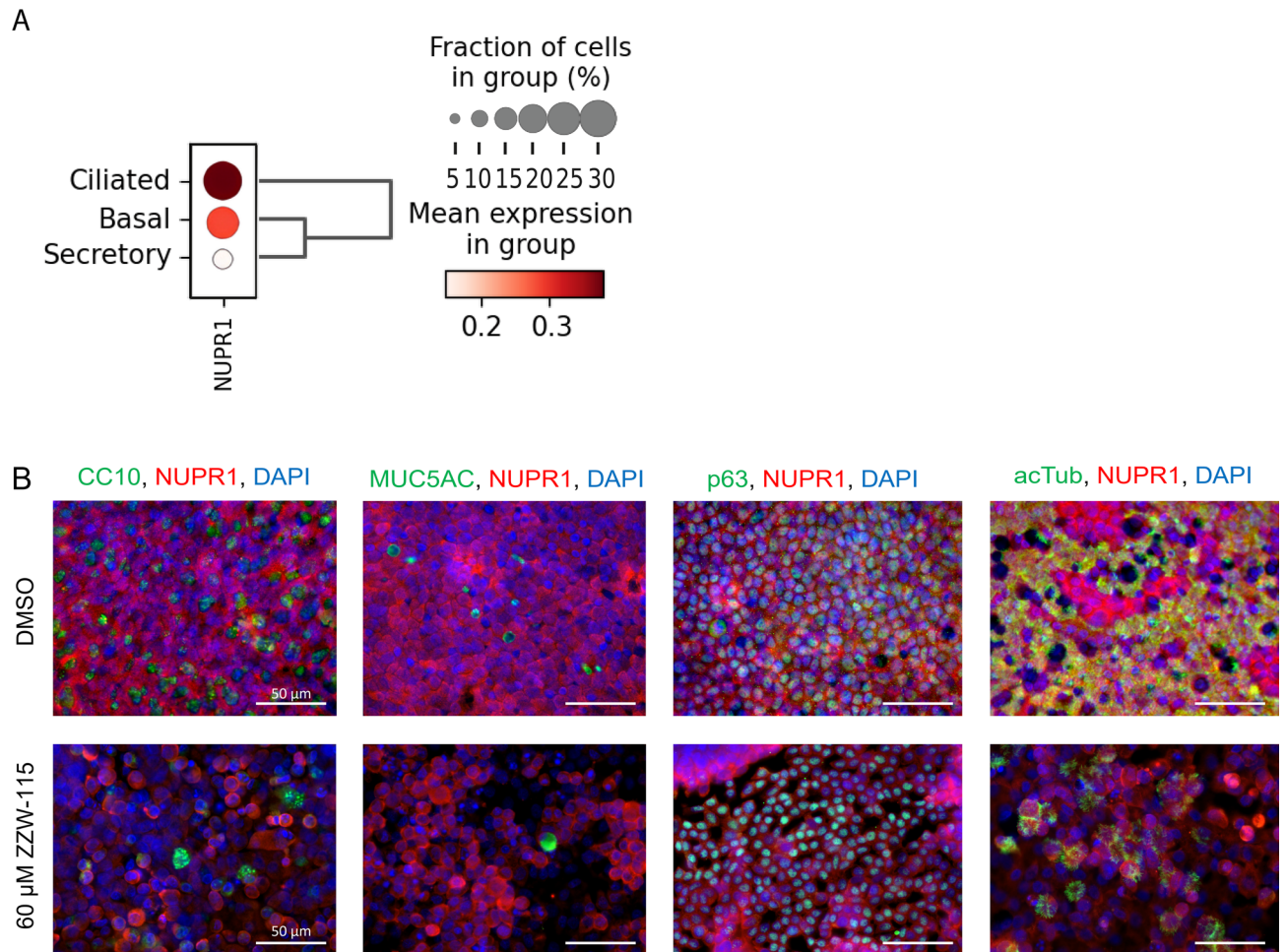


Fig. 3. Expression of *NUPR1* in fully differentiated phBECs is restricted to ciliated and basal cells. **(A)** Single-cell RNA sequencing (scRNA-seq) data of fully differentiated control phBECs ($n=2$) showed that ciliated and basal cells have the highest *NUPR1* expression. **(B)** Representative immunofluorescence of fully differentiated phBECs before and after *NUPR1*-inhibition with the *NUPR1*-inhibitor ZZW-115 at its IC_{50} of 60 μ M. The co-stainings of *NUPR1* with cell type-specific markers for secretory, basal, and ciliated cells (CC10/MUC5AC, secretory cells; p63, basal cells; acTub, ciliated cells) confirmed, that *NUPR1* is expressed in basal and ciliated cells in control ($n=4$). The stainings after ZZW-115 treatment show cell loss due to cell death after *NUPR1*-inhibition as well as the inhibition of nuclear translocation of *NUPR1* (scale bar 50 μ m).

Considerable loss of epithelial barrier integrity manifested at comparably lower ZZW-115 concentrations than cytotoxicity, indicating a strong protective effect of *NUPR1* in this context. Loss of epithelial barrier integrity was accompanied by considerable ZZW-115-induced cell detachment as visualized by light microscopy (Fig. 4I) and equally apparent in IF stainings (Fig. 3B).

To our surprise, and in contrast to the prediction by IPA, we found no evidence of increased *NUPR1* protein levels in cells exposed to CSE. In agreement with these findings, none of the IPA-predicted *NUPR1* target genes were changed in their expression upon CSE exposure on transcript level. Finally, prior CSE exposure did not significantly alter cytotoxicity, loss of cell barrier integrity and resulting cell loss induced by *NUPR1* inhibition. Collectively, while these findings establish an important role for *NUPR1* in bronchial cell viability, they provided no evidence for CS-induced activation of *NUPR1* in vitro and thus do not support a specific role for *NUPR1* in protecting bronchial epithelial cells from CS exposure-induced cell death.

Impact of *NUPR1* on ferroptosis and apoptosis in phBECs

Cell death due to *NUPR1* loss has been suggested to be induced through ferroptosis^{43–46}, apoptosis and necrosis^{47–49}, depending on cell type and context. To identify the mechanisms underlying the cytotoxic effects of the *NUPR1* inhibition in phBECs, we performed gene expression analysis of ferroptosis-related genes, lipid peroxidation assays, Annexin V/PI apoptosis/necrosis analysis and western blot analysis of ferroptosis and apoptosis-related genes. QPCR analysis revealed significant effects on expression of several ferroptosis-related genes upon *NUPR1* inhibition, including an increase in Acyl-CoA synthetase long chain family member 4 (*ACSL4*), Glutathione peroxidase 4 (*GPX4*) and Nuclear factor erythroid 2-related factor 2 (*NFE2L2*) and a decrease in Ferroptosis suppressor protein 1 (*FSP1*), Cystine/glutamate transporter (*SLC7A11*) and Heme

oxygenase 1 (*HO-1*) expression, while Glutamate-cysteine ligase catalytic subunit (*GCLC*) expression was not modulated (Fig. 5A–E, Supplemental Fig. S6). Of these targets, only *ACSL4* and *SLC7A11* were modulated by CSE. Lipid peroxidation assay with C11-Bodipy 581/591 was performed using flow cytometry. If peroxidation by lipid ROS in cells is occurring, the fluorescence is shifted from PE (reduced) to FITC (oxidized). Our analysis revealed no significant changes in the ratio of the FITC to PE channels, which represent the intracellular lipid peroxidation levels⁵⁰. Consequently, lipid peroxidation levels remained unchanged in control phBECs following ZZW-115 or CSE treatment (Fig. 5F), which was confirmed by western blot analysis for 4-hydroxynonenal (4HNE)-modified protein (Fig. 5G, H, Supplemental Fig. S7), an independent marker of lipid peroxidation. Finally, protein levels of GPX4 and *ACSL4* were not altered, neither by NUPR1 inhibition nor by CSE treatment (Fig. 5G, I, J, Supplemental Fig. S7).

Western blot analysis of cleaved caspase 3 showed a significant increase of cleaved caspase 3 and hence apoptosis upon inhibition of NUPR1 without CSE exposure (Fig. 5K, Supplemental Fig. S7). A similar trend was observed in the CSE-treated cells. In agreement with the previously observed cytotoxicity induced by ZZW-115, Annexin V/PI revealed a significant decrease of overall cell viability due to NUPR1 inhibition (Fig. 5L). No significant effect was seen for early apoptosis, late apoptosis or necrosis separately, but a consistent trend towards increase was observed for all three following ZZW-115 treatment (Supplemental Fig. S8). Collectively, these results demonstrate that NUPR1 protects phBECs from cell death in vitro and support a predominantly anti-apoptotic rather than an anti-ferroptotic role in this cell type, which is little affected by prior CSE exposure.

NUPR1 expression is lower in whole lung tissue of IPF patients compared to control

Airway and airway-like epithelial cells are emerging as key players in IPF aetiology²⁴ where the role of NUPR1, to the best of our knowledge, had not been addressed previously. Therefore, we investigated *NUPR1* expression in existing scRNA-seq datasets of four combined control and ILD cohorts (Munich, Chicago, Nashville, New Haven)²⁴. This revealed a decrease in *NUPR1* expression in overall lung tissue and also in bronchial epithelial cells in IPF compared to control (Fig. 6A, B). To test these findings, we performed IF stainings in whole lung tissue of IPF and control samples ($n=5$). These stainings also demonstrated a significant decrease of mean fluorescence intensity and hence *NUPR1* expression in IPF compared to control, both within the whole cells and nuclei (Fig. 6C–E). The scRNA-seq analysis revealed a decreased *NUPR1* expression in all cell types in IPF compared to control (Supplemental Fig. S9A). However, the difference in ciliated cells was marginal. *NUPR1* expression in IPF was highest in ciliated cells followed by basal cells and lowest in secretory cells of IPF-derived phBECs (Supplemental Fig. S9B).

To further assess the impact of CS on NUPR1, we separated *NUPR1* expression in the scRNA-seq dataset according to smoking history. Never and former smokers exhibited significantly higher *NUPR1* expression than active smokers in whole lung, as well as in bronchial epithelial cells (Supplemental Fig. S10). Despite being preliminary, these data indicate that CS exposure may suppress epithelial *NUPR1* expression in bronchial epithelial cells in vivo. Taken together, our findings based on patient lung specimens show that *NUPR1* expression is decreased in IPF and airway epithelial cells compared to control lung tissue and that active smoking decreases *NUPR1* expression. This indicates that chronic environmental exposures may trigger loss of epithelial NUPR1. Exploring whether this acute loss of NUPR1 in airway epithelial cells contributes to lung fibrogenesis is therefore a promising future research direction.

Following NUPR1 inhibition, IPF-derived phBECs are more susceptible to cell death than control phBECs

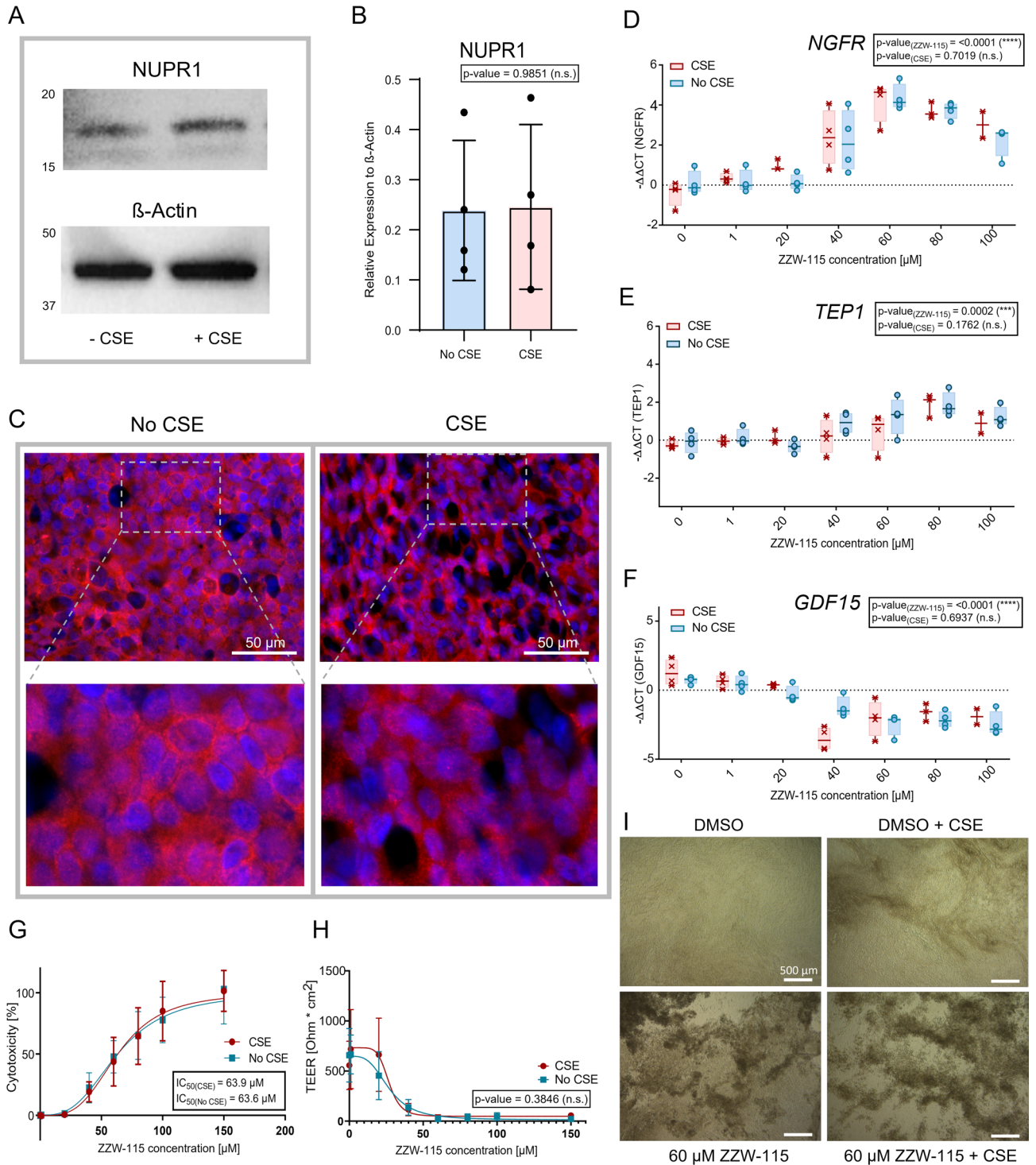
Following scRNA-analysis, which suggested a lower *NUPR1* expression in IPF-derived bronchial epithelial cells, we performed analysis in phBECs to investigate whether NUPR1 would protect from bronchial epithelial cell death also in IPF-derived cells. Therefore, cytotoxicity and epithelial barrier integrity were compared in control-derived and IPF-derived phBECs following NUPR1 inhibition by ZZW-115. Similar to control phBECs, NUPR1 inhibition with ZZW-115 increased cytotoxicity in a dose-dependent manner in IPF derived phBECs ($n=4$, Fig. 7A). However, IPF cells were more susceptible to ZZW-115-induced cell death, displaying a significantly lower IC_{50} value for ZZW-115 relative to control phBECs ($40.2 \pm 3.6 \mu\text{M}$ for IPF phBECs vs. $63.6 \pm 5.1 \mu\text{M}$ for control phBECs; Fig. 7B). Similar to our observations in control phBECs, these effects were not significantly modulated by prior CSE exposure of IPF-derived phBECs ($39.7 \pm 5.1 \mu\text{M}$ for IPF phBECs vs. $63.9 \pm 4.4 \mu\text{M}$ for control phBECs; Fig. 7C).

Furthermore, also in IPF-derived phBECs cell barrier integrity was significantly impaired in a dose-dependent manner (Fig. 7D), with no significant difference due to CSE exposure. Similar to control phBECs, significant loss of transepithelial electrical resistance occurred at comparably lower ZZW-115 concentrations than cytotoxicity in IPF-derived phBECs, suggesting a protective role of NUPR1 in cell barrier integrity.

NUPR1 expression overall is not consistently altered in IPF-derived relative to control phBECs, but IPF-derived bronchial epithelia show fewer ciliated cells

Given that IPF-derived phBECs were more susceptible to NUPR1 inhibition and scRNA-seq analysis suggested a decrease in *NUPR1* expression in IPF compared to control (Fig. 6A, B), we hypothesized that IPF-derived phBECs expressed less *NUPR1* than control phBECs. Western blot analysis revealed very heterogeneous protein levels of NUPR1 with a trend towards lower abundance in IPF-derived phBECs which, however, failed to reach significance. Prior CSE exposure again did not alter these protein levels (Fig. 8A–D, Supplemental Fig. S4).

Similar to control phBECs (Fig. 3B), NUPR1 clearly localized to basal and ciliated cells also in IPF-derived phBECs (Fig. 8E), consistent with the findings of the scRNA-seq analysis in IPF-derived bronchial epithelial cells (Supplemental Fig. S9B). To identify the cause of the increased susceptibility of IPF cells to NUPR1-dependent cytotoxicity, the cell populations in both groups were quantified from day 7 to day 28 of differentiation (Fig. 8F, G).



While the absolute cell number of NUPR1-positive cells was similar in both groups during the complete course of differentiation (Supplemental Fig. S11A), the analysis of individual cell types revealed a significantly lower number of ciliated cells and an increase in goblet cells in IPF-derived samples (Fig. 8H, I). The quantification of club and basal cells showed a trend towards an increase in IPF-derived cells, which, however, failed to reach significance (Supplemental Fig. S11B–C). Interestingly, this indicates that IPF-derived basal cells are intrinsically primed towards a secretory rather than a ciliated cell fate. Our observations suggest that ciliated cells play a more important role than basal cells in mediating the effects of NUPR1 inhibition in phBECs.

Discussion

To the best of our knowledge, this is the first study to investigate the intracellular proteomic effects of CS exposure in vitro in fully differentiated phBECs. Whereas several transcriptomic analyses have been reported^{51–55}, previous proteomic studies in this context were restricted to extracellular compartments including the secretome or exosomes and have only rarely been performed with primary human cells^{56–58}. Here, with the initial aim to

◀ **Fig. 4.** *NUPR1* in fully differentiated phBECs with and without cigarette smoke (CS) exposure. **(A)** Western blot analysis showed no significant difference in *NUPR1* protein level in control phBECs +/- CS exposure. β -actin was used as loading control. Uncropped western blot images are provided in Supplemental Fig. S4. **(B)** Quantification of *NUPR1* protein levels relative to β -actin ($n = 4$). **(C)** Immunofluorescence stainings of untreated control phBECs +/- CS revealed no difference in *NUPR1* localization (scale bar 50 μ m). **(D)** QPCR analysis of control phBECs ($n = 4$) treated with ZZW-115 (0–100 μ M) showed no significant impact on the expression of the IPA- suggested *NUPR1* target genes *NGFR*, **(E)** *TEP1* and **(F)** *GDF15* due to CS exposure. (Data for “No CSE” is identical to the data shown in Fig. 2B, D). **(G)** ZZW-115 increased cytotoxicity and **(H)** decreased cell barrier integrity in fully differentiated phBECs derived from control lungs ($n = 4$) in a dose-dependent manner, without a significant effect due to CS. Cytotoxicity was assessed with a lactate dehydrogenase assay and cell barrier integrity with transepithelial electrical resistance measurements. **(I)** *NUPR1* inhibition (60 μ M) caused cell loss in control phBECs to a similar extent with and without CS exposure (scale bar 500 μ m). [B one-way ANOVA followed by Tukey’s post hoc test for multiple comparisons; (D–F) two-way ANOVA test with multiple comparisons corrected by the two-stage step-up method of Benjamini, Krieger, and Yekutieli; (G–H) nonlinear regression without weighting was applied and the resulting curves of different conditions (+/- CS) were compared using an extra sum-of-squares *F*-test]. All data is presented as mean \pm SD.

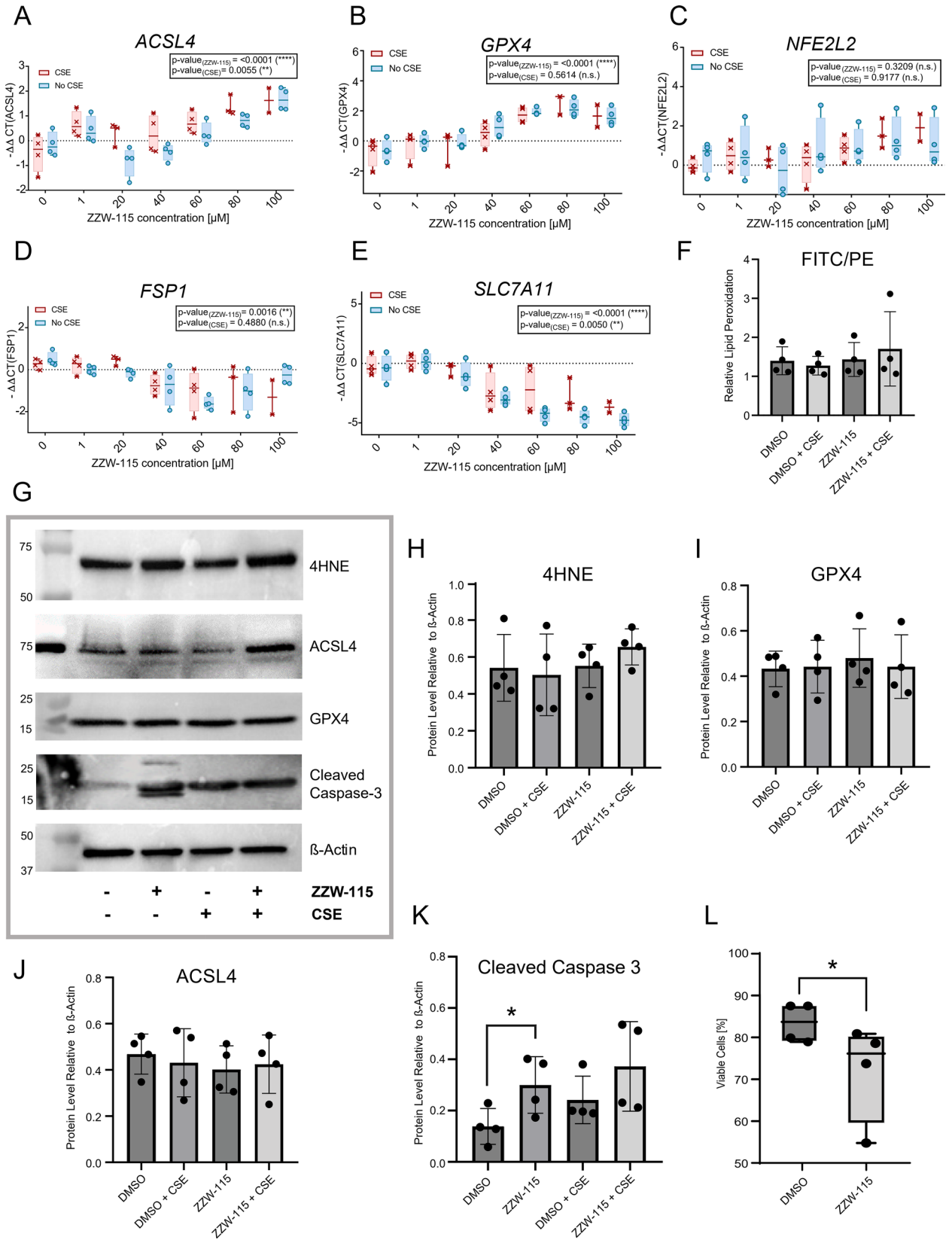
identify novel CS-induced key regulators in differentiated phBECs, we performed label-free proteomics followed by pathway enrichment analysis in a validated CS exposure model³⁰. The prediction of *NUPR1* activation by CS prompted us to study the cytoprotective role of *NUPR1* in control and IPF-derived phBECs. While our experimental results did not confirm activation of *NUPR1* by CS, our data clearly demonstrate a general protective, predominantly anti-apoptotic, role for *NUPR1* in bronchial epithelial cell death in vitro. Notably, *NUPR1* levels were lower in IPF whole lung including in bronchial epithelial cells in vivo, and IPF-derived phBECs in vitro were significantly more susceptible to *NUPR1* inhibition-induced cytotoxicity.

Pathway enrichment analysis revealed the activation of xenobiotic metabolism and other classical CS-induced pathways in response to chronic CS exposure, overall providing additional validation of our model. Notably, IL33 and SELH were identified as two of the most significantly down-regulated proteins following CS exposure (Fig. 1B, Supplemental Fig. S1–S2). Loss of IL33 is consistent with previous reports linking prolonged CS exposure to decreased *IL33* expression and release^{59,60}. This likely reflects a loss of IL33-producing basal cells and may contribute to the regeneration defects upon CSE exposure which we previously described in the same culture system⁶¹. Loss of SELH, a nuclear redox-regulating protein, in response to CS has not been reported previously and was most prominent at an early differentiation time point (day 7, Supplemental Fig. S1), which aligns with a role of SELH in protecting proliferating cells from oxidative stress^{62,63}. Although not the primary focus of this study, these findings warrant the future investigation of IL33 and SELH in the context of stem cell exhaustion and impaired regeneration following CS exposure.

NUPR1 (COM1/p8) is a stress-responsive transcriptional regulator which has been extensively studied in pancreatic disease and cancer^{39,44,46,48,64,65}, but comparatively little in the context of chronic lung disease. It has recently been reported that *NUPR1* expression is reduced in a subset of alveolar type II (AT2) epithelial cells in chronic obstructive pulmonary disease (COPD) and downregulated by CSE in the adenocarcinoma cell line A549⁴³. Therefore, the predicted activation of *NUPR1* by CS in our model was intriguing and given that its role in bronchial epithelial cells remained unexplored, we set out to investigate its function in this context. However, neither *NUPR1* protein levels nor nuclear translocation of *NUPR1* were changed upon CS exposure in phBECs. While inhibition of *NUPR1* by the specific inhibitor ZZW-115 dose-dependently decreased epithelial barrier integrity and induced cytotoxicity, none of these readouts were modulated by CS exposure in vitro. Hence, the IPA-derived hypothesis that CS would activate *NUPR1* in cultured phBECs was not supported by our follow-up analysis. These findings underscore the importance of experimentally validating computational pathway predictions which frequently are derived from unrelated tissue and molecular contexts. Nevertheless, all tested potential *NUPR1*-regulated targets were modulated as predicted by IPA in our culture system except for CEP170B, which confirms them as *NUPR1*-dependent targets also in human bronchial epithelial cells. However, it is important to mention that we cannot exclude the possibility that these findings are indirect and mediated through interactions with other transcription factors that are modulated through *NUPR1*-inhibition.

As increased cytotoxicity upon loss of *NUPR1* has been suggested to be mediated through ferroptosis^{43–46}, apoptosis and necrosis^{47–49}, depending on cell type and context, we assessed pro- and anti-ferroptotic readouts upon *NUPR1* inhibition in our culture system. Even though we observed altered ferroptosis-associated transcript levels upon *NUPR1* inhibition in phBECs (Fig. 5A–E, Supplemental Fig. S6), these were not translated to protein level (ACSL4, GPX4) and did not result in altered lipid peroxidation levels. As our CSE exposure did not significantly trigger ferroptosis, a stronger pro-ferroptotic stimulus may be necessary to reveal an anti-ferroptotic role of *NUPR1* in phBECs. Instead, our findings support a model where *NUPR1* protects bronchial epithelial cells from apoptosis: cleaved caspase 3 was significantly increased after *NUPR1* inhibition (Fig. 5K) and, even though early and late apoptosis were not significantly upregulated individually, as monitored by Annexin V/PI, both showed an increasing trend after *NUPR1* inhibition (Fig. 5L, Supplemental Fig. S8). Therefore, overall, our results agree with a predominantly anti-apoptotic role rather than an anti-ferroptotic role of *NUPR1* in phBECs but at the same time underscore the known context- and cell type-specific nature of *NUPR1*-dependent protective mechanisms^{47,64,66,67}.

Stress-induced airway epithelial cell pathways including apoptosis and increased vulnerability of the airway epithelium are increasingly recognized as an initiating factor in lung fibrogenesis^{24,68–70} but *NUPR1* had not



been studied in this context. Both scRNA-seq analyses as well as IF stainings in whole lung tissue (Fig. 6A–E) confirmed downregulation of NUPR1 in IPF relative to control lung tissue, including in bronchial epithelial cells. This prompted us to test the hypothesis that IPF-derived phBECs in vitro were more susceptible to NUPR1 inhibition. Notably, phBECs differentiated from IPF-derived basal cells mimicked typical properties of IPF airway epithelium including an increase in secretory cells and a loss of ciliated cells^{71,72}, indicating epigenetic reprogramming of airway basal cells that is maintained in culture⁶⁸. Also, the main NUPR1-expressing cell types

Fig. 5. NUPR1 modulation of ferroptosis and apoptosis. **(A)** QPCR analysis of control phBECs ($n=4$) treated with ZZW-115 (0–100 μM) revealed an increase in *ACSL4*, **(B)** *GPX4* and **(C)** *NFE2L2* and a decrease in **(D)** *FSP1* and **(E)** *SLC7A11* due to NUPR1 inhibition, with a significant effect of cigarette smoke (CS) on *ACSL4* and *SLC7A11*. **(F)** Lipid peroxidation assay of control phBECs (+/- CS, $n=4$) treated with DMSO or ZZW-115 (60 μM) was performed using flow cytometry. The quantification showed no significant modulation in the ratio of the FITC to PE channels, which represent the intracellular lipid peroxidation levels. Consequently, lipid peroxidation was not modulated in any condition. **(G)** Western blot analysis of control phBECs (+/- CS, $n=4$) treated with DMSO and ZZW-115 (60 μM) did not show any significant modulation in the protein levels of **(H)** 4HNE-modified protein, **(I)** *GPX4* or **(J)** *ACSL4*, confirming that NUPR1 inhibition does not induce ferroptosis in our culture model. Uncropped images are provided in Supplemental Fig. S7. **(K)** Western blot analysis of control phBECs (+/- CS, $n=4$) treated with DMSO or ZZW-115 (60 μM) revealed a significant increase ($p=0.0471$ *) of cleaved caspase 3 on protein levels due to NUPR1 inhibition. However, this effect was not significant in the CS treated condition. **(L)** Flow cytometry of control phBECs ($n=4$) treated with DMSO or ZZW-115 (60 μM) using Annexin IV/PI showed a significant decrease ($p=0.0470$) of overall cell viability (Annexin V-negative/PI-negative cells) due to NUPR1 inhibition. [A–E two-way ANOVA with multiple comparisons corrected by the two-stage step-up method of Benjamini, Krieger, and Yekutieli; F, H–L repeated-measures one-way ANOVA followed by Tukey's post hoc test for multiple comparisons]. All data is presented as mean \pm SD.

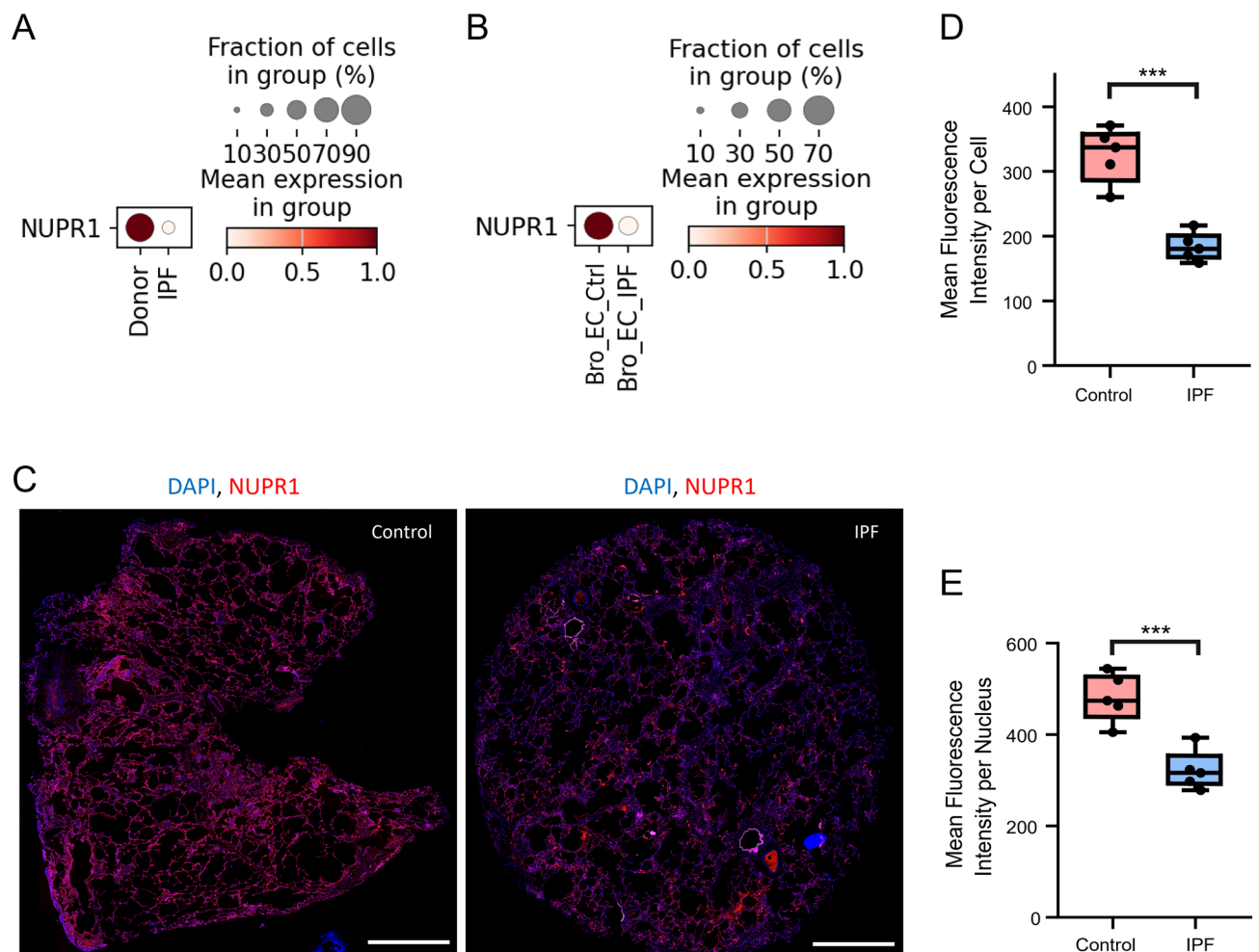


Fig. 6. Single cell RNA sequencing (scRNA-seq) and immunofluorescence analysis of NUPR1 in IPF and control samples. **(A)** ScRNA-seq of four combined cohorts showed a higher *NUPR1* expression in IPF compared to control ("Ctrl") in whole lung and **(B)** bronchial epithelial cells ("Bro_EC"). **(C)** Representative immunofluorescence stainings of a control and IPF lung sample (scale bar 2000 μm). **(D)** Quantification of NUPR1 mean fluorescence intensity in DAPI-positive cells and **(E)** nuclei of IPF and control lung samples ($n=5$) revealed a significantly lower expression in IPF samples in both comparisons. The quantification was performed with QuPath 0.5.1. A two-tailed unpaired t -test revealed a significantly lower *NUPR1* expression in IPF cells ($p=0.0002$) and IPF nuclei ($p=0.0009$) compared to control. All data is presented as mean \pm SD.

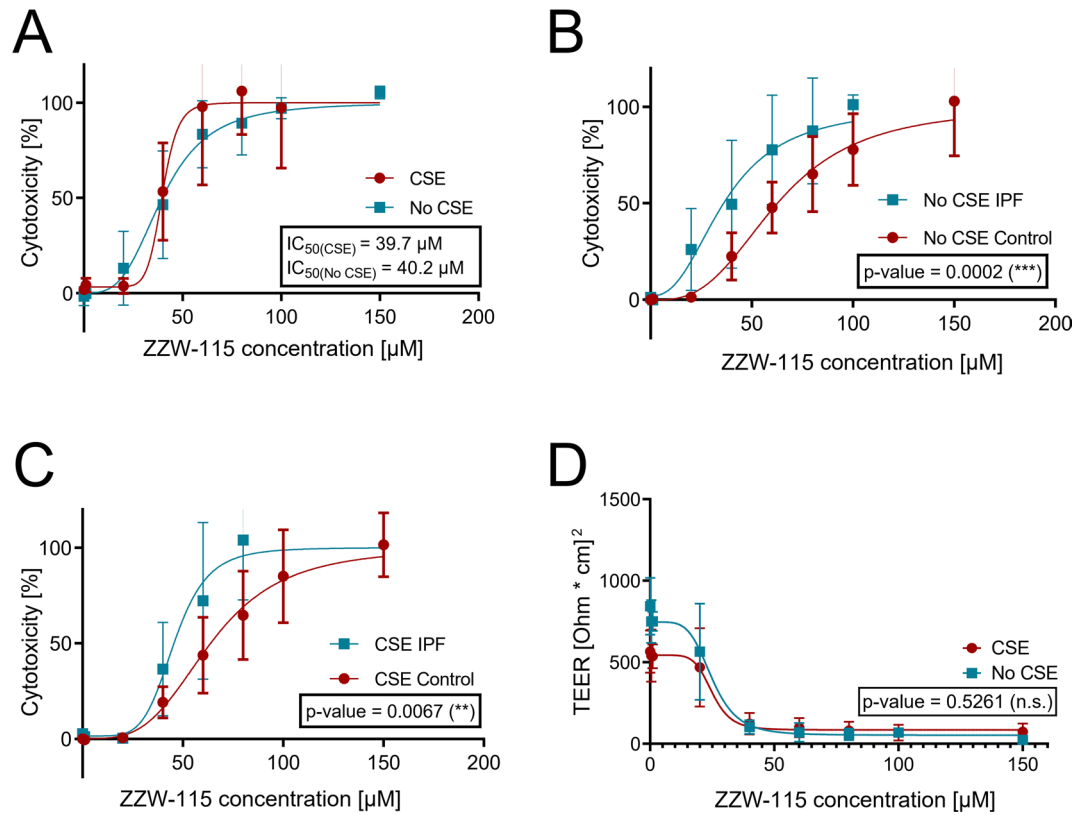
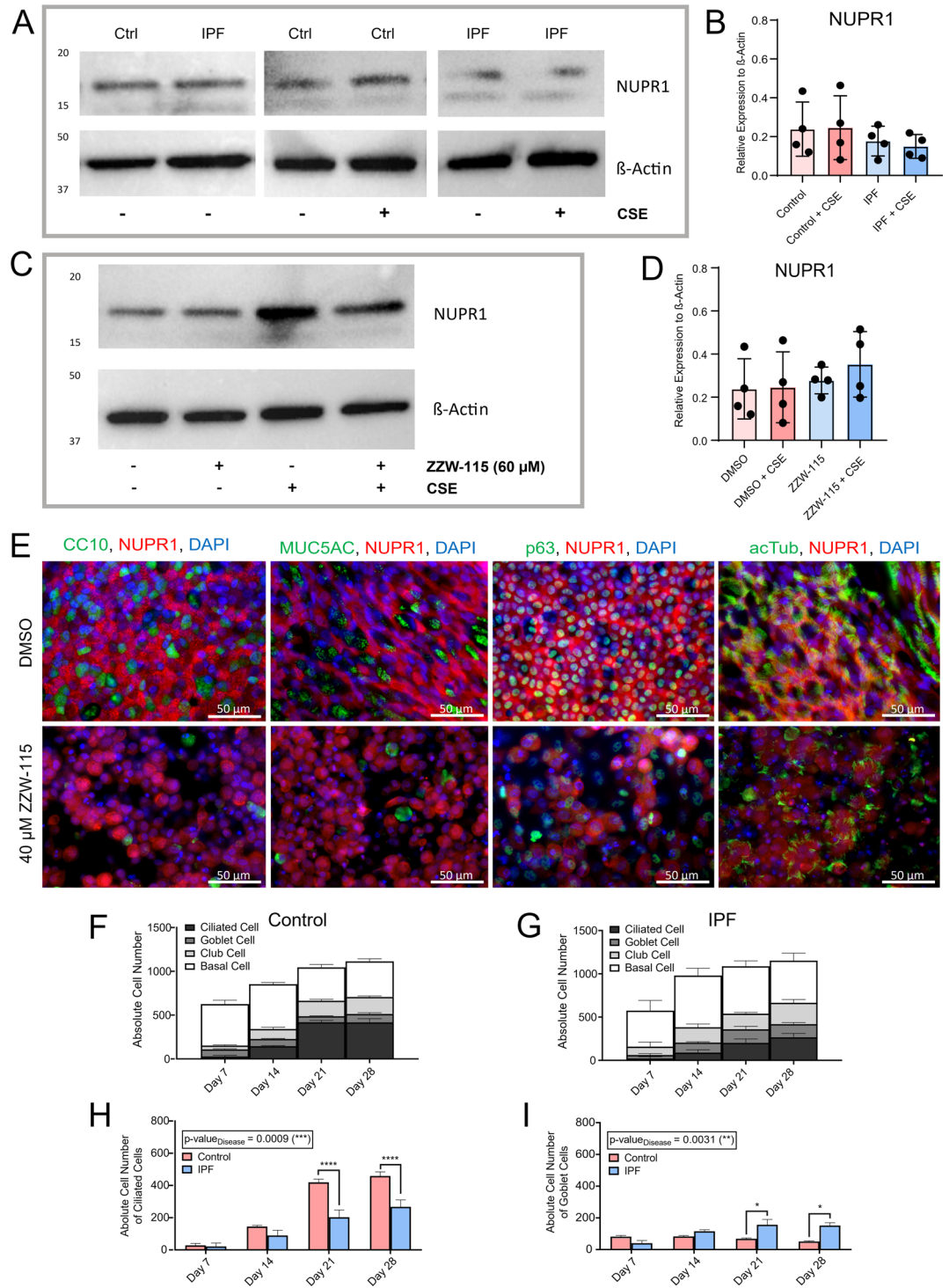


Fig. 7. Higher susceptibility to NUPR1 inhibition-induced cytotoxicity in IPF phBECs. **(A)** Lactate dehydrogenase cytotoxicity assay revealed dose-dependent cytotoxicity for the NUPR1 inhibitor ZZW-115 (0–150 μM) in IPF-derived phBECs, both with and without prior CS treatment ($n = 4$). **(B, C)** The IC_{50} -values were lower in IPF-derived cells relative to control phBECs, both **(B)** with and **(C)** without CS-treatment compared to control. **(D)** NUPR1 inhibition decreased TEER in fully differentiated phBECs derived from IPF-patients ($n = 4$) in a dose-dependent manner, again unaltered by prior CS exposure. For the analysis of these data, nonlinear regression without weighting was applied and the resulting curves of different conditions (+/- CS, control vs. IPF) were compared using an extra sum-of-squares F-test. All data is presented as mean \pm SD.

in vitro, *i.e.* basal and ciliated cells, reflected the ones in IPF (Supplemental Fig. S9). Even if loss of NUPR1 protein was not fully recapitulated in IPF-derived vs. control phBECs in vitro, IPF-derived cells were indeed considerably more susceptible to NUPR1 inhibition, demonstrating significantly lower IC_{50} values for ZZW-115 (Fig. 7B, C). As NUPR1 expression was at best marginally reduced in IPF-derived phBECs in our study, the increased susceptibility to NUPR1 inhibition likely reflects more nuanced mechanisms. One contributing factor may be differences in cell-type composition, as IPF cultures contained fewer ciliated and more secretory cells (Fig. 8E–I), suggesting that basal and/or secretory progenitor populations may be more vulnerable to NUPR1 inhibition than ciliated cells. Furthermore, IPF-derived epithelial cells are generally more injury-prone due to impaired barrier integrity, elevated ER stress, mitochondrial dysfunction, and increased oxidative stress, all of which reduce resilience to external insults^{73–76}. Taken together, these mechanisms may explain the enhanced sensitivity of IPF-derived phBECs to NUPR1 inhibition despite largely preserved NUPR1 expression.

NUPR1 is emerging as a potential target in oncology, including for lung cancer^{66,77,78}, because NUPR1 supports survival, therapy resistance, and stress adaptation of tumor cells^{64,79,80}; pharmacologic blockade with ZZW-115 suppresses tumour growth and angiogenesis and sensitizes cancer cells to cytotoxic stress^{39,49,81}. Our data indicate that NUPR1 is cytoprotective in bronchial epithelium including in IPF-derived cells, raising a safety concern that systemic or airway-exposed NUPR1 inhibitors could cause epithelial cell death and potentially trigger or exacerbate lung fibrosis. Notably, lung cancer and IPF frequently co-occur and share risk factors like age and CS; IPF confers an independently elevated risk of lung cancer and worse outcomes^{82–84}. This underscores the need for caution when considering NUPR1 inhibition in cancer patients with fibrotic lung disease.

Our study has several limitations. Our data clearly indicate the involvement of NUPR1 in several mechanisms in phBECs. However, we cannot exclude the possibility that these observed NUPR1-induced effects are indirect and mediated through interactions with other stress-responsive transcription factors or proteins that are modulated via NUPR1-inhibition. Additionally, a conclusive assessment of a protective role from CS exposure-induced cell death would require NUPR1 activation or overexpression experiments. As no specific NUPR1 agonist is currently available and overexpression approaches are technically challenging in fully differentiated phBECs, further studies will be needed to address this question. Moreover, generating fully differentiated phBEC cultures is time-consuming, resource-intensive, and costly, which inherently constrains sample size and



experimental depth. Primary cells are known to exhibit a high inter-donor variability and, with an $n=4-5$, our study may therefore in part have been underpowered to detect some of the CSE-related changes. Additionally, our in vitro model lacks the complex multicellular and immune environment as well as mechanical forces in the lung, which play a crucial role in lung fibrogenesis and fibrosis progression. Future research using co-culture models of phBECs with fibroblasts or immune cells, such as alveolar macrophages, could possibly provide deeper insights into the role of NUPR1. The used culture conditions are generally optimised for cell viability and contain a variety of growth factors, which may influence *NUPR1* expression as well as IPF-specific characteristics, such as the loss of NUPR1. Finally, we used basal cells derived from the proximal bronchi, not distal airway progenitor cells or cells from honeycomb cysts, which are thought to play a more important role in IPF in vivo. Nevertheless, several key observations in our model, including the reduced number of ciliated cells, the increase in secretory cells, and a loss of cellular resilience in IPF-derived phBECs, are consistent with reported epithelial alterations in IPF in vivo, supporting the value of our model as a meaningful platform for mechanistic investigation^{71,72}.

◀ **Fig. 8.** NUPR1 in IPF-derived primary human bronchial epithelial cells (phBECs). **(A)** Western blot analysis of control and IPF-derived phBECs (+/- cigarette smoke (CS), $n=4$) did not show any significant difference in the protein levels of NUPR1. β -actin was used as loading control. **(B)** Quantification of NUPR1 protein levels relative to β -actin. **(C)** Western blot analysis of control phBECs (+/- CS, $n=4$) did not show any significant difference in the protein levels of NUPR1 before and after NUPR1 inhibition. The comparison was conducted between treatments with vehicle control (DMSO) and 60 μ M NUPR1-inhibitor ZZW-115 (close to its IC_{50} in control cells). β -actin was used as loading control. **(D)** Quantification of NUPR1 protein levels relative to β -actin. **(E)** Representative immunofluorescence of fully differentiated IPF-derived phBECs before and after NUPR1-inhibition with the NUPR1-inhibitor ZZW-115 at its IC_{50} of 40 μ M. The co-stainings of NUPR1 with cell type-specific markers for secretory, basal, and ciliated cells (CC10/MUC5AC, secretory cells; p63, basal cells; acTub, ciliated cells) confirmed, that NUPR1 is expressed in basal and ciliated cells in IPF ($n=4$). The stainings after ZZW-115 treatment show cell loss due to cell death after NUPR1 inhibition as well as the inhibition of nuclear translocation of NUPR1 (scale bar 50 μ m). **(F)** Absolute cell count of the cell type specific quantification of differentiating control and **(G)** IPF-derived phBECs ($n=4$) at day 7, 14, 21 and 28 at air-liquid interface. Statistical analysis was by two-way ANOVA with multiple comparisons corrected by the two-stage step-up method of Benjamini, Krieger. **(H, I)** Absolute cell type quantification of **(H)** ciliated and **(I)** goblet cells in control and IPF-derived phBECs at day 7, 14, 21 and 28 revealed a significant decrease especially at later timepoints in IPF samples. [B, D repeated-measures one-way ANOVA followed by Tukey's post hoc test for multiple comparisons; (F–I) two-way ANOVA with multiple comparisons corrected by the two-stage step-up method of Benjamini, Krieger]. All data is presented as mean \pm SD.

Conclusion

In conclusion, we present the first intracellular proteomic analysis of CS exposure in fully differentiated phBECs, identifying NUPR1 as a candidate regulator of epithelial stress responses. Our results confirm cell type- and tissue-specific differences in NUPR1-dependent pathways and emphasize the need for context-dependent validation of pathway enrichment analysis predictions. Although NUPR1 was not activated by CS in vitro, specific inhibition of NUPR1 nuclear translocation demonstrated that NUPR1 exerts a predominantly anti-apoptotic and cytoprotective role in phBECs. Importantly, NUPR1 is lost in IPF and IPF-derived epithelial cells were significantly more sensitive to NUPR1 inhibition, suggesting that loss of NUPR1-mediated survival mechanisms in the IPF airway epithelium may contribute to disease pathogenesis. Together, these findings position NUPR1 as a context-dependent epithelial stress regulator with potential relevance for epithelial vulnerability in IPF and warrant further investigation into its therapeutic modulation. Furthermore, our study uncovers novel CS-induced reductions in IL33 and SELH, highlighting additional pathways potentially involved in epithelial exhaustion and impaired regeneration.

Data availability

The mass spectrometry proteomics data have been deposited to the ProteomeXchange Consortium via the PRIDE²⁸ partner repository with the dataset identifier PXD063763. All other data supporting the findings of this study are available within the paper and its Supplementary Information.

Received: 28 November 2025; Accepted: 28 April 2026

Published online: 11 May 2026

References

1. Glass, D. S. et al. Idiopathic pulmonary fibrosis: Molecular mechanisms and potential treatment approaches. *Respir. Investig.* **58**(5), 320–335. <https://doi.org/10.1016/j.resinv.2020.04.002> (2020).
2. Raghu, G. et al. Diagnosis of idiopathic pulmonary fibrosis. An official ATS/ERS/JRS/ALAT clinical practice guideline. *Am. J. Respir. Crit. Care Med.* **198**(5), e44–e68. <https://doi.org/10.1164/rccm.201807-1255ST> (2018).
3. Fang, M., He, B. & Xiao, J. Smoking and idiopathic pulmonary fibrosis: A meta-analysis. *Nicotine Tob. Res.* **26**(12), 1599–1606. <https://doi.org/10.1093/ntr/ntae100> (2024).
4. Richeldi, L. et al. Efficacy and safety of nintedanib in idiopathic pulmonary fibrosis. *N. Engl. J. Med.* **370**(22), 2071–2082. <https://doi.org/10.1056/NEJMoa1402584> (2014).
5. King, T. E. et al. A phase 3 trial of pirfenidone in patients with idiopathic pulmonary fibrosis. *N. Engl. J. Med.* **370**(22), 2083–2092. <https://doi.org/10.1056/NEJMoa1402582> (2014).
6. Richeldi, L. et al. Nerandomilast in patients with idiopathic pulmonary fibrosis. *N. Engl. J. Med.* **392**(22), 2193–2202. <https://doi.org/10.1056/NEJMoa2414108> (2025).
7. Bae, W. et al. Impact of smoking on the development of idiopathic pulmonary fibrosis: Results from a nationwide population-based cohort study. *Thorax* **77**(5), 470–476. <https://doi.org/10.1136/thoraxjnl-2020-215386> (2022).
8. Baumgartner, K. B., Samet, J. M., Stidley, C. A., Colby, T. V. & Waldron, J. A. Cigarette smoking: A risk factor for idiopathic pulmonary fibrosis. *Am. J. Respir. Crit. Care Med.* **155**(1), 242–248. <https://doi.org/10.1164/ajrccm.155.1.9001319> (1997).
9. Douglas, D. et al. Tobacco smoking is associated with combined pulmonary fibrosis and emphysema and worse outcomes in interstitial lung disease. *Am. J. Physiol. Lung Cell. Mol. Physiol.* **325**(2), L233–L243. <https://doi.org/10.1152/ajplung.00083.2023> (2023).
10. Kaul, B. et al. Epidemiology of idiopathic pulmonary fibrosis among U.S. Veterans, 2010–2019. *Ann. Am. Thorac. Soc.* **19**(2), 196–203. <https://doi.org/10.1513/AnnalsATS.202103-295OC> (2022).
11. Ryu, J. H., Colby, T. V., Hartman, T. E. & Vassallo, R. Smoking-related interstitial lung diseases: A concise review. *Eur. Respir. J.* **17**(1), 122–132. <https://doi.org/10.1183/09031936.01.17101220> (2001).
12. Yoon, H.-Y., Kim, H., Bae, Y. & Song, J. W. Smoking status and clinical outcome in idiopathic pulmonary fibrosis: A nationwide study. *Respir. Res.* **25**(1), 191. <https://doi.org/10.1186/s12931-024-02819-w> (2024).

13. Chen, T.-Y. et al. Conditioned media of adipose-derived stem cells suppresses sidestream cigarette smoke extract induced cell death and epithelial-mesenchymal transition in lung epithelial cells. *Int. J. Mol. Sci.* <https://doi.org/10.3390/ijms222112069> (2021).
14. WHO Tobacco. <https://www.who.int/news-room/fact-sheets/detail/tobacco>. Accessed 25 Mrz 2025 (31.07.2023).
15. Banks, E. et al. Tobacco smoking and all-cause mortality in a large Australian cohort study: Findings from a mature epidemic with current low smoking prevalence. *BMC Med.* **13**, 38. <https://doi.org/10.1186/s12916-015-0281-z> (2015).
16. Doll, R., Peto, R., Boreham, J. & Sutherland, I. Mortality in relation to smoking: 50 years' observations on male British doctors. *BMJ (Clin. Res. Ed.)* **328**(7455), 1519. <https://doi.org/10.1136/bmj.38142.554479.AE> (2004).
17. Siddiqi, K. et al. Global burden of disease due to smokeless tobacco consumption in adults: An updated analysis of data from 127 countries. *BMC Med.* **18**(1), 222. <https://doi.org/10.1186/s12916-020-01677-9> (2020).
18. Hiemstra, P. S., McCray, P. B. & Bals, R. The innate immune function of airway epithelial cells in inflammatory lung disease. *Eur. Respir. J.* **45**(4), 1150–1162. <https://doi.org/10.1183/09031936.00141514> (2015).
19. Schamberger, A. C., Staab-Weijnitz, C. A., Mise-Racek, N. & Eickelberg, O. Cigarette smoke alters primary human bronchial epithelial cell differentiation at the air-liquid interface. *Sci. Rep.* **5**, 8163. <https://doi.org/10.1038/srep08163> (2015).
20. Davis, J. D. & Wypych, T. P. Cellular and functional heterogeneity of the airway epithelium. *Mucosal Immunol.* **14**(5), 978–990. <https://doi.org/10.1038/s41385-020-00370-7> (2021).
21. Huukkanen, J., Pelkonen, O., Hakkola, J. & Raunio, H. Expression and regulation of xenobiotic-metabolizing cytochrome P450 (CYP) enzymes in human lung. *Crit. Rev. Toxicol.* **32**(5), 391–411. <https://doi.org/10.1080/20024091064273> (2002).
22. Park, Y., Ahn, C. & Kim, T.-H. Occupational and environmental risk factors of idiopathic pulmonary fibrosis: A systematic review and meta-analyses. *Sci. Rep.* **11**(1), 4318. <https://doi.org/10.1038/s41598-021-81591-z> (2021).
23. Wolters, P. J., Collard, H. R. & Jones, K. D. Pathogenesis of idiopathic pulmonary fibrosis. *Annu. Rev. Pathol. Mech. Dis.* **9**, 157–179. <https://doi.org/10.1146/annurev-pathol-012513-104706> (2014).
24. Chakraborty, A., Mastalerz, M., Ansari, M., Schiller, H. B. & Staab-Weijnitz, C. A. Emerging roles of airway epithelial cells in idiopathic pulmonary fibrosis. *Cells* <https://doi.org/10.3390/cells11061050> (2022).
25. Adegunsoye, A. et al. Genetics and genomics of pulmonary fibrosis: Charting the molecular landscape and shaping precision medicine. *Am. J. Respir. Crit. Care Med.* **210**(4), 401–423. <https://doi.org/10.1164/rccm.202401-0238SO> (2024).
26. Evans, C. M. et al. Idiopathic pulmonary fibrosis: A genetic disease that involves mucociliary dysfunction of the peripheral airways. *Physiol. Rev.* **96**(4), 1567–1591. <https://doi.org/10.1152/physrev.00004.2016> (2016).
27. Zöllner, M. et al. Quantitative proteomics identifies nuclear protein 1 as a regulator of cell death in differentiated primary human bronchial epithelial cells. *Am. J. Respir. Crit. Care Med.* **211**, A6855–A6855. <https://doi.org/10.1164/ajrccm.2025.211.Abstracts.A6855> (2025).
28. Perez-Riverol, Y. et al. The PRIDE database at 20 years: 2025 update. *Nucleic Acids Res.* **53**(D1), D543–D553. <https://doi.org/10.1093/nar/gkae1011> (2025).
29. Berthold, E. J. et al. Effects of immunophilin inhibitors and non-immunosuppressive analogs on coronavirus replication in human infection models. *Front. Cell. Infect. Microbiol.* **12**, 958634. <https://doi.org/10.3389/fcimb.2022.958634> (2022).
30. Mastalerz, M. et al. Validation of in vitro models for smoke exposure of primary human bronchial epithelial cells. *Am. J. Physiol. Lung Cell. Mol. Physiol.* **322**(1), L129–L148. <https://doi.org/10.1152/ajplung.00091.2021> (2022).
31. Nakayama, M. et al. Quantitative proteomics of differentiated primary bronchial epithelial cells from chronic obstructive pulmonary disease and control identifies potential novel host factors post-influenza A virus infection. *Front. Microbiol.* **13**, 957830. <https://doi.org/10.3389/fmicb.2022.957830> (2022).
32. Jaeger, B. et al. Airway basal cells show a dedifferentiated KRT17high phenotype and promote fibrosis in idiopathic pulmonary fibrosis. *Nat. Commun.* **13**(1), 5637. <https://doi.org/10.1038/s41467-022-33193-0> (2022).
33. Lang, N. J. et al. Ex vivo tissue perturbations coupled to single-cell RNA-seq reveal multilineage cell circuit dynamics in human lung fibrogenesis. *Sci. Transl. Med.* **15**(725), eadh0908. <https://doi.org/10.1126/scitranslmed.adh0908> (2023).
34. Rico de Souza, A. et al. The aryl hydrocarbon receptor attenuates acute cigarette smoke-induced airway neutrophilia independent of the dioxin response element. *Front. Immunol.* **12**, 630427. <https://doi.org/10.3389/fimmu.2021.630427> (2021).
35. Beane, J. et al. SIRT1 pathway dysregulation in the smoke-exposed airway epithelium and lung tumor tissue. *Cancer Res.* **72**(22), 5702–5711. <https://doi.org/10.1158/0008-5472.Can-12-1043> (2012).
36. Tian, D., Zhu, M., Li, J., Ma, Y. & Wu, R. Cigarette smoke extract induces activation of beta-catenin/TCF signaling through inhibiting GSK3beta in human alveolar epithelial cell line. *Toxicol. Lett.* **187**(1), 58–62. <https://doi.org/10.1016/j.toxlet.2009.02.002> (2009).
37. Zuo, H. et al. A-kinase anchoring proteins diminish TGF-β1/cigarette smoke-induced epithelial-to-mesenchymal transition. *Cells* <https://doi.org/10.3390/cells9020356> (2020).
38. Ogawa, F. et al. Role of KRAS in regulating normal human airway basal cell differentiation. *Respir. Res.* **20**(1), 181. <https://doi.org/10.1186/s12931-019-1129-4> (2019).
39. Lan, W. et al. ZZW-115-dependent inhibition of NUPR1 nuclear translocation sensitizes cancer cells to genotoxic agents. *JCI Insight* <https://doi.org/10.1172/jci.insight.138117> (2020).
40. Santofimia-Castaño, P. et al. Targeting the stress-induced protein NUPR1 to treat pancreatic adenocarcinoma. *Cells* <https://doi.org/10.3390/cells8111453> (2019).
41. Stoleriu, M. G. et al. COPD basal cells are primed towards secretory to multiciliated cell imbalance driving increased resilience to environmental stressors. *Thorax* **79**(6), 524–537. <https://doi.org/10.1136/thorax-2022-219958> (2024).
42. Decramer, M., Janssens, W. & Miravittles, M. Chronic obstructive pulmonary disease. *Lancet (London Engl.)* **379**(9823), 1341–1351. [https://doi.org/10.1016/S0140-6736\(11\)60968-9](https://doi.org/10.1016/S0140-6736(11)60968-9) (2012).
43. Sauler, M. et al. Characterization of the COPD alveolar niche using single-cell RNA sequencing. *Nat. Commun.* **13**(1), 494. <https://doi.org/10.1038/s41467-022-28062-9> (2022).
44. Huang, C., Santofimia-Castaño, P. & Iovanna, J. NUPR1: A critical regulator of the antioxidant system. *Cancers* <https://doi.org/10.3390/cancers13153670> (2021).
45. Huang, C. et al. NUPR1 inhibitor ZZW-115 induces ferroptosis in a mitochondria-dependent manner. *Cell Death Discov.* **7**(1), 269. <https://doi.org/10.1038/s41420-021-00662-2> (2021).
46. Liu, J. et al. NUPR1 is a critical repressor of ferroptosis. *Nat. Commun.* **12**(1), 647. <https://doi.org/10.1038/s41467-021-20904-2> (2021).
47. Santofimia-Castaño, P. & Iovanna, J. Combating pancreatic cancer chemoresistance by triggering multiple cell death pathways. *Pancreatol. Off J. Int. Assoc. Pancreat.* **21**(3), 522–529. <https://doi.org/10.1016/j.pan.2021.01.010> (2021).
48. Santofimia-Castaño, P. et al. Inactivation of NUPR1 promotes cell death by coupling ER-stress responses with necrosis. *Sci. Rep.* **8**(1), 16999. <https://doi.org/10.1038/s41598-018-35020-3> (2018).
49. Santofimia-Castaño, P. et al. Ligand-based design identifies a potent NUPR1 inhibitor exerting anticancer activity via necroptosis. *J. Clin. Invest.* **129**(6), 2500–2513. <https://doi.org/10.1172/JCI127223> (2019).
50. Borst, J. W., Visser, N. V., Kouptsova, O. & Visser, A. J. Oxidation of unsaturated phospholipids in membrane bilayer mixtures is accompanied by membrane fluidity changes. *Biochim. Biophys. Acta (BBA) Mol. Cell Biol. Lipids* **1487**(1), 61–73. [https://doi.org/10.1016/s1388-1981\(00\)00084-6](https://doi.org/10.1016/s1388-1981(00)00084-6) (2000).
51. Glass, K. et al. Integrative epigenomic analysis in differentiated human primary bronchial epithelial cells exposed to cigarette smoke. *Sci. Rep.* **8**(1), 12750. <https://doi.org/10.1038/s41598-018-30781-3> (2018).

52. Mathis, C. et al. Human bronchial epithelial cells exposed in vitro to cigarette smoke at the air-liquid interface resemble bronchial epithelium from human smokers. *Am. J. Physiol. Lung Cell. Mol. Physiol.* **304**(7), L489–503. <https://doi.org/10.1152/ajplung.00181.2012> (2013).
53. Shen, Y., Wolkowicz, M. J., Kotova, T., Fan, L. & Timko, M. P. Transcriptome sequencing reveals e-cigarette vapor and mainstream smoke from tobacco cigarettes activate different gene expression profiles in human bronchial epithelial cells. *Sci. Rep.* **6**, 23984. <https://doi.org/10.1038/srep23984> (2016).
54. van der Does, A. M. et al. Early transcriptional responses of bronchial epithelial cells to whole cigarette smoke mirror those of in vivo exposed human bronchial mucosa. *Respir. Res.* **23**(1), 227. <https://doi.org/10.1186/s12931-022-02150-2> (2022).
55. Xiong, R. et al. Integration of transcriptome analysis with pathophysiological endpoints to evaluate cigarette smoke toxicity in an in vitro human airway tissue model. *Arch. Toxicol.* **95**(5), 1739–1761. <https://doi.org/10.1007/s00204-021-03008-0> (2021).
56. Candiano, G. et al. Proteomic analysis of the airway surface liquid: Modulation by proinflammatory cytokines. *Am. J. Physiol. Lung Cell Mol. Physiol.* **292**(1), L185–L198. <https://doi.org/10.1152/ajplung.00085.2006> (2007).
57. Mossina, A. et al. Cigarette smoke alters the secretome of lung epithelial cells. *Proteomics* <https://doi.org/10.1002/pmic.201600243> (2017).
58. Sanchez-Guzman, D. et al. Long-term evolution of the epithelial cell secretome in preclinical 3D models of the human bronchial epithelium. *Sci. Rep.* **11**(1), 6621. <https://doi.org/10.1038/s41598-021-86037-0> (2021).
59. Faiz, A. et al. IL-33 expression is lower in current smokers at both transcriptomic and protein levels. *Am. J. Respir. Crit. Care Med.* **208**(10), 1075–1087. <https://doi.org/10.1164/rccm.202210-1881OC> (2023).
60. Pace, E. et al. Cigarette smoke alters IL-33 expression and release in airway epithelial cells. *Biochim. Biophys. Acta Mol. Basis Dis.* **1842**(9), 1630–1637. <https://doi.org/10.1016/j.bbadis.2014.06.009> (2014).
61. Chakraborty, A. et al. Development of a Polidocanol-based human in vitro model to explore airway epithelial repair. *Am. J. Respir. Cell Mol. Biol.* <https://doi.org/10.1165/rcmb.2024-0117OC> (2025).
62. Bertz, M. et al. Selenoprotein H controls cell cycle progression and proliferation of human colorectal cancer cells. *Free Radic. Biol. Med.* **127**, 98–107. <https://doi.org/10.1016/j.freeradbiomed.2018.01.010> (2018).
63. Wu, R. T. Y., Cao, L., Chen, B. P. C. & Cheng, W.-H. Selenoprotein H suppresses cellular senescence through genome maintenance and redox regulation. *J. Biol. Chem.* **289**(49), 34378–34388. <https://doi.org/10.1074/jbc.M114.611970> (2014).
64. Cano, C. E., Hamidi, T., Sandi, M. J. & Iovanna, J. L. Nupr1: The Swiss-knife of cancer. *J. Cell. Physiol.* **226**(6), 1439–1443. <https://doi.org/10.1002/jcp.22324> (2011).
65. Mallo, G. V. et al. Cloning and expression of the rat p8 cDNA, a new gene activated in pancreas during the acute phase of pancreatitis, pancreatic development, and regeneration, and which promotes cellular growth. *J. Biol. Chem.* **272**(51), 32360–32369. <https://doi.org/10.1074/jbc.272.51.32360> (1997).
66. Guo, X. et al. Lentivirus-mediated RNAi knockdown of NUPR1 inhibits human nonsmall cell lung cancer growth in vitro and in vivo. *Anat. Rec. (Hoboken)* **295**(12), 2114–2121. <https://doi.org/10.1002/ar.22571> (2012).
67. Li, J. et al. Knockdown of NUPR1 inhibits the proliferation of glioblastoma cells via ERK1/2, p38 MAPK and caspase-3. *J. Neurooncol.* **132**(1), 15–26. <https://doi.org/10.1007/s11060-016-2337-0> (2017).
68. Bridges, J. P. et al. Progressive lung fibrosis: Reprogramming a genetically vulnerable bronchoalveolar epithelium. *J. Clin. Invest.* <https://doi.org/10.1172/JCI183836> (2025).
69. Chen, G. et al. XBP1S regulates MUC5B in a promoter variant-dependent pathway in idiopathic pulmonary fibrosis airway epithelia. *Am. J. Respir. Crit. Care Med.* **200**(2), 220–234. <https://doi.org/10.1164/rccm.201810-1972OC> (2019).
70. Park, S.-Y. et al. Club cell-specific role of programmed cell death 5 in pulmonary fibrosis. *Nat. Commun.* **12**(1), 2923. <https://doi.org/10.1038/s41467-021-23277-8> (2021).
71. Herrera, J. A. et al. Morphologically intact airways in lung fibrosis have an abnormal proteome. *Respir. Res.* **24**(1), 99. <https://doi.org/10.1186/s12931-023-02400-x> (2023).
72. Peng, Y. et al. Mucus hypersecretion and ciliary impairment in conducting airway contribute to alveolar mucus plugging in idiopathic pulmonary fibrosis. *Frontiers Cell Dev Biol.* **9**, 810842. <https://doi.org/10.3389/fcell.2021.810842> (2021).
73. Camelo, A., Dunmore, R., Sleeman, M. A. & Clarke, D. L. The epithelium in idiopathic pulmonary fibrosis: Breaking the barrier. *Front. Pharmacol.* **4**, 173. <https://doi.org/10.3389/fphar.2013.00173> (2014).
74. Lawson, W. E. et al. Endoplasmic reticulum stress in alveolar epithelial cells is prominent in IPF: Association with altered surfactant protein processing and herpesvirus infection. *Am. J. Physiol. Lung Cell. Mol. Physiol.* **294**(6), L1119–L1126. <https://doi.org/10.1152/ajplung.00382.2007> (2008).
75. Tanjore, H., Lawson, W. E. & Blackwell, T. S. Endoplasmic reticulum stress as a pro-fibrotic stimulus. *Biochim. Biophys. Acta* **1832**(7), 940–947. <https://doi.org/10.1016/j.bbadis.2012.11.011> (2013).
76. Zou, J. et al. Idiopathic pulmonary fibrosis is associated with tight junction protein alterations. *Biochim. Biophys. Acta Biomembr.* **1862**(5), 183205. <https://doi.org/10.1016/j.bbmem.2020.183205> (2020).
77. Li, Y. et al. Combination of AAV-mediated NUPR1 knockdown and trifluoperazine induces premature senescence in human lung adenocarcinoma A549 cells in nude mice. *Oncol. Rep.* **43**(2), 681–688. <https://doi.org/10.3892/or.2020.7455> (2020).
78. Wang, L. et al. Knockdown of NUPR1 inhibits angiogenesis in lung cancer through IRE1/XBP1 and PERK/eIF2 α /ATF4 signaling pathways. *Open Med. (Wars)* **18**(1), 20230796. <https://doi.org/10.1515/med-2023-0796> (2023).
79. Giroux, V. et al. p8 is a new target of gemcitabine in pancreatic cancer cells. *Clin. Cancer Res.* **12**(1), 235–241. <https://doi.org/10.1158/1078-0432.CCR-05-1700> (2006).
80. Murphy, A. & Costa, M. Nuclear protein 1 imparts oncogenic potential and chemotherapeutic resistance in cancer. *Cancer Lett.* **494**, 132–141. <https://doi.org/10.1016/j.canlet.2020.08.019> (2020).
81. Lan, W. et al. Targeting NUPR1 with the small compound ZZW-115 is an efficient strategy to treat hepatocellular carcinoma. *Cancer Lett.* **486**, 8–17. <https://doi.org/10.1016/j.canlet.2020.04.024> (2020).
82. Ballester, B., Milara, J. & Cortijo, J. Idiopathic pulmonary fibrosis and lung cancer: Mechanisms and molecular targets. *Int. J. Mol. Sci.* <https://doi.org/10.3390/ijms20030593> (2019).
83. Brown, S.-A. W. et al. Idiopathic pulmonary fibrosis and lung cancer. A systematic review and meta-analysis. *Ann. Am. Thorac. Soc.* **16**(8), 1041–1051. <https://doi.org/10.1513/AnnalsATS.201807-481OC> (2019).
84. Kirkil, G., Mogulkoc, N. & Jovanovic, D. Risk factors and management of lung cancer in idiopathic pulmonary fibrosis: A comprehensive review. *Sarcoidosis Vasc. Diffuse Lung Dis.* **42**(1), 15604. <https://doi.org/10.36141/svldl.v42i1.15604> (2025).

Acknowledgements

We gratefully acknowledge the provision of human biomaterial (phBECs from control/non-chronic lung disease- and IPF-patients and FFPE sections of peritumoral tissue) and clinical data from the CPC-M bioArchive and its partners at the Asklepios Biobank Gauting, the LMU Hospital and the Ludwig-Maximilians-Universität München. We thank the patients and their families for their support.

Author contributions

CAS-W and MZ conceived and designed the study. MZ, MM, ED, JMP, EH, AC, MN, MK, AJ, MGS, SMH and HS performed experiments and acquired data. MZ, MM, JMP, EH, SRSP, AC, MN, MK, HM, RLG, AJ, SMH,

HS, and CAS-W analyzed and interpreted the data. LJDS, WAW, BMV, AP, BJ, PSC, AH, AÖY provided essential resources for this study and patient material. MZ and CAS-W prepared the manuscript for submission. All authors have read, edited, and approved the final manuscript.

Funding

This work was supported by the Helmholtz Association, the German Center for Lung Research (DZL), the German Research Foundation (Deutsche Forschungsgemeinschaft, DFG) within the Research Training Group GRK2338 (CAS-W, HS, AÖY), a faculty start-up package from the University of Colorado School of Medicine awarded to CAS-W, and a Marie Skłodowska-Curie postdoctoral fellowship awarded to MN.

Declarations

Competing interests

The authors declare no competing interests.

Additional information

Supplementary Information The online version contains supplementary material available at <https://doi.org/10.1038/s41598-026-51510-1>.

Correspondence and requests for materials should be addressed to C.A.S.-W.

Reprints and permissions information is available at www.nature.com/reprints.

Publisher's note Springer Nature remains neutral with regard to jurisdictional claims in published maps and institutional affiliations.

Open Access This article is licensed under a Creative Commons Attribution 4.0 International License, which permits use, sharing, adaptation, distribution and reproduction in any medium or format, as long as you give appropriate credit to the original author(s) and the source, provide a link to the Creative Commons licence, and indicate if changes were made. The images or other third party material in this article are included in the article's Creative Commons licence, unless indicated otherwise in a credit line to the material. If material is not included in the article's Creative Commons licence and your intended use is not permitted by statutory regulation or exceeds the permitted use, you will need to obtain permission directly from the copyright holder. To view a copy of this licence, visit <http://creativecommons.org/licenses/by/4.0/>.

© The Author(s) 2026